PAPER

Collective effects of organic molecules based on the Holstein–Tavis–Cummings model

IOP Publishing Journal of Physics B: Atomic, Molecular and Optical Physics
J. Phys. B: At. Mol. Opt. Phys. **54** (2021) 145101 (14pp) https://doi.org/10.1088/1361-6455/ac0afa

Collective effects of organic molecules based on the Holstein–Tavis–Cummings model

Quansheng Zhang[1,*] **and Ke Zhang**[2,3]

[1] Beijing Computational Science Research Center, Beijing 100193, People's Republic of China
[2] Helmholtz Institute Mainz, GSI Helmholtzzentrum für Schwerionenforschung, 55099 Mainz, Germany
[3] Johannes Gutenberg-University Mainz, 55099 Mainz, Germany

E-mail: qshzhang@csrc.ac.cn

Received 9 April 2021, revised 18 May 2021
Accepted for publication 14 June 2021
Published 13 August 2021

Abstract

We study the collective effects of an ensemble of organic molecules confined in an optical cavity based on the Holstein–Tavis–Cummings model. By using the quantum Langevin approach and adiabatically eliminating the degree of freedom of the vibrational motion, we analytically obtain the expression of the cavity transmission spectrum to analyze the features of polaritonic states. As an application, we show that the dependence of the frequency shift of the lower polaritonic state on the number of molecules can be used in the detection of the ultra-cold molecules. We also numerically analyze the fluorescence spectrum. The variation of the spectral profile with various numbers of molecules provides signatures for the modification of molecular conformation.

Keywords: Holstein–Tavis–Cummings model, quantum optics, Langevin approach, collective effects

(Some figures may appear in colour only in the online journal)

1. Introduction

The interaction between molecules and light has played an important role in photochemical reactivity [1], molecular spectroscopy [2, 3], chemical fingerprinting [4], and the generation of non-classical states of light [5]. When molecules are located in an optical cavity, the coupling strength can be enhanced [6–9]. In the strong coupling regime, the energy may oscillate between molecules and the cavity field at a faster rate than their relaxation rates, inducing hybridization of the molecular and photonic states into polaritonic states [10]. In this situation, the potential energy landscape for the molecular conformation will be modified, giving rise to a range of further effects on the material properties of the molecules. As the modifications for molecular conformation are tunable, it has opened up new routes for the control of chemical reactivity [11, 12], energy and charge transport [13, 14], and Förster resonance energy transfer [15–17]. Besides, the modifications for molecular conformation will have an influence on the profiles of molecular absorption and fluorescence spectra [18]. For the electronic transitions, the coupling between the electronic state and the molecular conformation will lead to the structure of the emission (or absorption) spectra observed in experiments [9, 19] with multiple peaks. The observable molecular spectra will provide signatures for the variation of molecular conformation.

To provide an understanding of such phenomena, the Holstein–Tavis–Cummings (HTC) model has been widely adopted to describe the light-electronic-vibration problem [18, 20]. Furthermore, an approach based on the quantum Langevin equation to solve the HTC model has been developed recently [17]. It provides an alternative path to understand the Stokes and anti-Stokes processes [17], the Purcell effect

* Author to whom any correspondence should be addressed.

under the influence of the phononic environments [21], and the Floquent engineering [22] at the level of operators rather than states. However, the previous works [17, 21, 22] mainly focus on a single molecule. When multiple molecules are confined in a cavity, the system will experience more complex dynamics. When many molecules are introduced to couple a quantized cavity field, an efficient interaction between molecules will be induced, leading to collective effects [23]. On the other hand, the description of the electronic transition dressed by the vibrational motion suggests that the vibrators for one molecule will be coupled to that for other molecules. Considering the above facts, a profound influence will be brought upon the polaritonic states, as well as the fluorescence (or absorption) spectrum.

Inspired by this, we provide here a further study of the HTC model when multiple molecules are presented. Going from a set of coupled standard Langevin equations for the whole system, and adiabatically eliminating the degree of freedom of the vibrational motion, a set of effective equations can be derived, involving the average values of Pauli operators, photonic operators, and their correlations. From these equations, we study the collective effects in the optical cavity via the cavity transmission spectrum, the steady population, and the fluorescence spectrum. To test the reasonableness of approximation, we perform a numerical simulation for the case of two molecules in the limit of weak coupling between the electronic states and molecular conformation using the QuTiP package [24], and also undertake perturbative treatment in the first order to compare against the perturbative method in the second order for general situations. We show that the profiles of the cavity transmission spectrum and the fluorescence spectrum can be modified via the number of molecules, which will provide signatures of the modification of molecular conformation. Such phenomena will provide potential applications in the detection of ultra-cold molecules [25], as well as the control of chemical reactions [12, 26], energy and charge transport [14, 20], and so on. In contrast, we also present the analysis of a special case in the limit without the coupling between electronic states and molecular conformation, i.e. the Tavis–Cummings (TC) model.

The structure of this paper is organized as follows. In section 2, we describe the model and give the formal solution for the average value of the Pauli lowering operator with the adiabatic elimination for the degree of freedom vibrational motion. In section 3, we investigate the influence of the number of molecules on the polaritonic features via the cavity transmitted field for the HTC model and TC model, respectively. In section 4, we analyze the influence of the number of molecules on the fluorescence spectrum for the HTC model and TC model, respectively. Finally, a summary is given in section 5.

2. Model

As illustrated in figure 1, the proposed system of interest consists of an ensemble of N organic molecules, which are confined in a Fabry–Perot microcavity. Considering the organic molecules comprised of z atoms, there will be $3z-6$ (or $3z-5$ for linear molecules) normal modes of vibration in the configuration space of the nuclear coordinates [11, 20]. When describing a chemical reaction, often a few of these modes, which are associated with the reaction coordinates, are investigated [11, 20, 27]. For a single reaction coordinate, one can assume that the vibrational frequencies for the ground and excited electronic states are the same. Thus, the system can be represented as a two-level system (corresponding to its ground $|g_m\rangle$ and excited $|e_m\rangle$ electric states) and a phonon mode (denoting the harmonic vibrational degree of freedom with the annihilation operator b_m). Here, each molecule is labeled with the index m (running from 1 to N). The dynamic for a single free molecule is then governed by the Holstein Hamiltonian [20]

$$H_m = \nu b_m^\dagger b_m + [\omega_e + \lambda\nu(b_m + b_m^\dagger)]\sigma_m^\dagger\sigma_m, \qquad (1)$$

where $\omega_e = \omega_{00} + \lambda^2\nu$ is the effective transition frequency, with ω_{00} being the bare splitting between the ground and excited electric states, and ν is the vibrational frequency for the harmonic oscillator. The parameter λ is related to the Huang–Rhys factor S, i.e. $S = \lambda^2$. Here, S ranges from 0 to ~ 2 [28–30], resulting from the displacement of the equilibrium position of the vibrational mode between the excited and ground electronic states. Furthermore, λ also characterizes the coupling between the electronic states and molecular conformation. In the limit of $\lambda = 0$, one can simplify the system for the molecule described by equation (1) to be a two-level system.

When the cavity field is single-mode, the molecule–cavity interaction can be depicted by the TC Hamiltonian

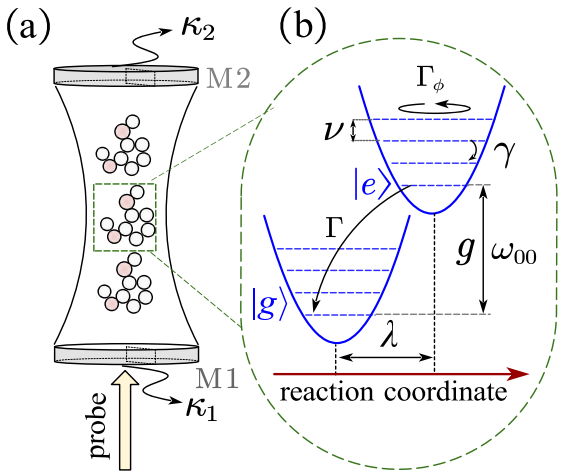

Figure 1. Model schematics. (a) An ensemble of N organic molecules are placed inside a Fabry–Perot microcavity with a single mode. The dissipation for the cavity field occurs at rates κ_1 through the mirror M1 and κ_2 through the mirror M2. (b) A diagram of molecular level structure and relaxation processes. Each molecule is represented by two harmonic oscillator potential surfaces of two electronic states with the shift λ in the reaction coordinate. The cavity field resonantly couples to the electronic transition $|g\rangle \leftrightarrow |e\rangle$ with the coupling strength g. The relaxation processes of each molecule include the electronic decay at rate Γ, the pure dephasing at rate Γ_ϕ, and internal vibrational relaxation at rate γ.

(we set $\hbar = 1$)

$$H_{\rm int} = \omega_c a^\dagger a + g\sum_{m=1}^{N}(a^\dagger\sigma_m + {\rm H.c.}), \tag{2}$$

where the operator a annihilates a cavity photon at frequency ω_c, $\sigma_m = |g_m\rangle\langle e_m|$ annihilates the molecular excitation, and g is the coupling strength for a single molecule. Notably, this Hamiltonian implies the assumption that all molecules are equally coupled to the cavity field by neglecting the influences resulting from the disorder of transition dipole moments of molecules and molecular spatial distribution. Such an approximation will conveniently provide a qualitative description of the collective behavior of organic polaritons [31].

Taking into account the free part of the molecules and the situation in which the cavity is probed by a classical field at frequency ω_l with the coupling strength η, the total Hamiltonian for such a system in the rotating wave approximation can be given

$$H = \sum_{m}^{N} H_m + H_{\rm int} + i\eta(a{\rm e}^{{\rm i}\omega_l t} - a^\dagger{\rm e}^{-{\rm i}\omega_l t}). \tag{3}$$

Applying a polaron transformation $H_{\rm p} = U^\dagger H U$ with

$$U = \exp\left[\sum_{m}^{N}\lambda\sigma_m^\dagger\sigma_m(b_m - b_m^\dagger)\right], \tag{4}$$

one can recast the Hamiltonian (3) into

$$\begin{aligned} H_{\rm p} = &\sum_{m}^{N}(\nu b_m^\dagger b_m + \omega_{00}\sigma_m^\dagger\sigma_m) + \omega_c a^\dagger a \\ &+ \left(\sum_{m}^{N} g\mathcal{D}_m^\dagger\sigma_m a^\dagger + i\eta{\rm e}^{{\rm i}\omega_l t}a + {\rm H.c.}\right), \end{aligned} \tag{5}$$

where $\mathcal{D}_m = \exp[\lambda(b_m - b_m^\dagger)]$ is a displaced operator for the mth molecule. In this representation, the coupling between the two-level system and cavity field is dressed by vibrations via the Frank–Condon factors ${}_{\rm vib}\langle n|\mathcal{D}|m\rangle_{\rm vib}$ for the transition $|g\rangle|n\rangle_{\rm vib} \to |e\rangle|m\rangle_{\rm vib}$, where $|n\rangle_{\rm vib}$ (or $|m\rangle_{\rm vib}$) are Fock states of vibrations.

To model the open system, we should consider the relaxation processes as depicted in figure 1(b), including the loss of the cavity field at rate $\kappa = \kappa_1 + \kappa_2$ (encompassing losses via both mirrors), the spontaneous emission of the electronic transition at rate Γ, and the pure dephasing of the electronic transition at rate Γ_ϕ. Their effects are described as Lindblad terms, and are represented by $\mathcal{L}_{\gamma_\mathcal{O}}[\mathcal{O}] = \gamma_\mathcal{O}(2\mathcal{O}\rho\mathcal{O}^\dagger - \mathcal{O}^\dagger\mathcal{O}\rho - \rho\mathcal{O}^\dagger\mathcal{O})$ with a collapse operator $\mathcal{O}$ and a corresponding decay rate $\gamma_\mathcal{O}$. Finally, the dynamics of the system can be described by a master equation of the density matrix ρ

$$\begin{aligned} \dot\rho = &-i[H,\rho] + \mathcal{L}_\kappa[a] + \sum_{m}^{N}\mathcal{L}_{\Gamma_\phi}[\sigma_m^\dagger\sigma_m - \sigma_m\sigma_m^\dagger] \\ &+ \sum_{m}^{N}\mathcal{L}_\Gamma[\sigma_m] + \sum_{m}^{N}\mathcal{L}_\gamma[b_m]. \end{aligned} \tag{6}$$

The last term in equation (6) represents the vibrational relaxation process at rate γ. Physically, when considering the coupling between the vibrator and a reservoir of phonons (also described as a Brownian noise dissipation model [17, 21]) in a solvent or surrounding medium, the vibrational relaxation of molecules cannot be simply expressed in Lindblad form [21, 22, 32]. In this work, for the purposes of discussion, we still adopt the Lindblad decay model to describe the vibrational relaxation process. This approach has been used in several theoretical studies to explore molecular spectroscopy [17, 22], the Purcell effect [21], energy transfer [17], and organic polariton lasing [33]. In the limit $\lambda^2\gamma \ll \Gamma$, the Lindblad decay model for the vibrational relaxation will be indistinguishable to the Brownian noise model [17, 22]. Additionally, the spontaneous emission is also involved in the vibrational motion, which can be ignored due to the fact that its decay rate is much smaller than the vibrational relaxation rate γ.

The master equation method is usually equivalent to the Langevin approach. For the given master equation in the Lindblad form, described as $\mathcal{L}_{\gamma_\mathcal{O}}[\mathcal{O}]$ with a collapse operator $\mathcal{O}$ and decay rate $\gamma_\mathcal{O}$, we can map it onto a Langevin form [34] as

$$\begin{aligned} \frac{{\rm d}}{{\rm d}t}\mathcal{A} = &\, i[H,\mathcal{A}] - \sum_j\left[\mathcal{A},\mathcal{O}_j^\dagger\right]\left\{\gamma_{\mathcal{O}_j}\mathcal{O}_j - \sqrt{2\gamma_{\mathcal{O}_j}}\mathcal{O}_j^{\rm in}\right\} \\ &+ \sum_j\left\{\gamma_{\mathcal{O}_j}\mathcal{O}_j^\dagger - \sqrt{2\gamma_j}\mathcal{O}_j^{{\rm in}\dagger}\right\}[\mathcal{A},\mathcal{O}_j], \end{aligned} \tag{7}$$

with an arbitrary system operator $\mathcal{A}$ and any collapse operator $\mathcal{O}_j$ in the set $\{b_m, \sigma_m, \sigma_m^\dagger\sigma_m - \sigma_m\sigma_m^\dagger, a\}$.

Under the conditions of weak driving $\eta \ll \kappa$, the cavity field in the steady situation will have much less one photon and the molecules will largely stay in the electronic ground state, i.e. $\sigma_m^\dagger\sigma_m \ll 1$. In the rotating frame at the probe frequency ω_l, the quantum Langevin equations for the cavity field a and polarized operator $\tilde\sigma_m = \mathcal{D}_m^\dagger\sigma_m$ are given as [17]

$$\begin{aligned} \frac{{\rm d}}{{\rm d}t}a = &-(i\Delta_c + \kappa)a - ig\sum_{m}^{N}\sigma_m + \sqrt{2\kappa_1}A_{\rm in} \\ &+ \sqrt{2\kappa_2}a_2^{\rm in}(t), \end{aligned} \tag{8a}$$

$$\frac{{\rm d}}{{\rm d}t}\tilde\sigma_m \approx -(i\Delta + \Gamma_\perp)\tilde\sigma_m - ig\mathcal{D}_m^\dagger a + \sqrt{2\Gamma_\perp}\mathcal{D}_m^\dagger\sigma_m^{\rm in}, \tag{8b}$$

with the detuning $\Delta_c = \omega_c - \omega_l$ and $\Delta = \omega_{00} - \omega_l$. Here, $\Gamma_\perp = \Gamma + 2\Gamma_\phi$ is the effective transverse relaxation rate. Notably, under the description of the vibrational relaxation in the Lindblad form, additional dephasing of the polarized operator will occur. However, we can neglect such dephasing as this will lead to the disagreement with experimental observations of lifetime of the electronic transition [17, 21, 22]. Additionally, $A_{\rm in}(t) = \eta/\sqrt{2\kappa_1} + a_1^{\rm in}(t)$ denotes the effective cavity input with zero-average input noise $a_1^{\rm in}(t)$. Here, we assume that the temperature of the cavity field is zero, i.e. $T_{\rm cav} = 0$, then the non-vanishing correlation $\langle a_1^{\rm in}(t)a_1^{{\rm in}\dagger}(t')\rangle = \delta(t-t')$ and $\langle a_2^{\rm in}(t)a_2^{{\rm in}\dagger}(t')\rangle = \delta(t-t')$ will be obtained. The electronic transition is also affected by a white nose input $\sigma_m^{\rm in}$ with non-zero correlation $\langle\sigma_m^{\rm in}(t)\sigma_n^{{\rm in}\dagger}(t')\rangle = \delta_{mn}\delta(t-t')$.

Then, we can formally integrate equation (8*b*) to get the solution of $\tilde{\sigma}_m$ and, subsequently, of the Pauli lowering operator

$$\sigma_m(t) = -\int_0^t \mathrm{d}t_1\, \mathrm{e}^{-(\mathrm{i}\Delta+\Gamma_\perp)(t-t_1)}\mathcal{D}_m(t)\mathcal{D}_m^\dagger(t_1)\,[iga(t_1) - \sqrt{2\Gamma_\perp}\sigma_m^{\mathrm{in}}(t_1)\Big] + \mathrm{e}^{-(\mathrm{i}\Delta+\Gamma_\perp)t}\mathcal{D}_m(t)\mathcal{D}_m^\dagger(0)\sigma_m(0). \tag{9}$$

In a solvent or surrounding medium, the coupling between the vibrator and a reservoir of phonons will lead to a large relaxation rate for vibrational motion (i.e. $\gamma \gg \Gamma_\perp$) [21, 32, 35]. Additionally, we also assume that the vibrational relaxation rate is much larger than the cavity field (i.e. $\gamma \gg \kappa$). Under these conditions, the timescale of vibrational relaxation will be much shorter than that for the relaxation of the electronic state, and also the decay of the cavity field. Therefore, the vibrational state may be considered to be in the steady state [32]. By treating the vibrations as a Markovian phonon bath [32, 36], the degrees of freedom of the cavity field and vibrational motion can be separated as

$$\langle a(t_1)\mathcal{D}_m(t)\mathcal{D}_m^\dagger(t_1)\rangle \approx \langle a(t_1)\rangle\langle \mathcal{D}_m(t)\mathcal{D}_m^\dagger(t_1)\rangle, \tag{10}$$

as well as that for Pauli lowering operators and vibrational motion

$$\langle \sigma_n(t_1)\mathcal{D}_m(t)\mathcal{D}_m^\dagger(t_1)\rangle \approx \langle \sigma_n(t_1)\rangle\langle \mathcal{D}_m(t)\mathcal{D}_m^\dagger(t_1)\rangle. \tag{11}$$

If these molecules are initially prepared in the ground electronic state, and zero photon populated in the cavity, the last term in equation (9) will be canceled when we take the average over the cavity field, the vibrational motion, and the electronic state. Finally, the average dipole moment $\langle\sigma_m\rangle$ can be derived

$$\langle\sigma_m\rangle = -ig\int_0^\infty \mathrm{d}t_1 \mathcal{F}_m(t-t_1)\langle a(t_1)\rangle, \tag{12}$$

with the definition $\mathcal{F}_m(t-t_1) = \Theta(t-t_1)\exp[-(i\Delta + \Gamma_\perp)(t-t_1)]\langle\mathcal{D}_m(t)\mathcal{D}_m^\dagger(t_1)\rangle$, where $\Theta(t)$ is the Heaviside step function. The two-time correlation for the displacement operators $\langle\mathcal{D}_m(t)\mathcal{D}_m^\dagger(t_1)\rangle$ can be expressed as (at $t > t_1$)

$$\langle\mathcal{D}_m(t)\mathcal{D}_m^\dagger(t_1)\rangle = e^{-\lambda^2}e^{\lambda^2 e^{-(\gamma+i\nu)(t-t_1)}}, \tag{13}$$

when the effective vibrational temperature satisfies $k_\mathrm{B}T_{\mathrm{vib}}/\hbar\nu \ll 1$ (see appendix A). The important quantity to be emphasized is the function $\langle\mathcal{D}_m(t)\mathcal{D}_m^\dagger(t_1)\rangle$, which implies the influence of the vibrational mode on the excitons in organic molecules. When $\lambda = 0$, one can achieve the value of the function $\langle\mathcal{D}_m(t)\mathcal{D}_m^\dagger(t_1)\rangle = 1$. Then, the interaction between electronic states and molecular conformation will be removed. For finite λ, the coupling between the vibrational mode and the excitons will result in some new fascinating physics.

Notably, the Pauli operator can feed back into itself via the cavity field, resulting in higher-order correlation between the displaced operators. The adiabatic approximation depicted by equation (13) has neglected the contributions from these higher-order correlations. To explore the influence of these higher-order correlations, we discuss further in appendices B and C.

3. Cavity transmission

For the molecule–cavity system discussed in the previous section, the electronic transition will be dressed by vibrational motion with the coupling between the electronic states and molecular conformation.

In the limit of large vibrational relaxation (i.e. $\gamma \gg \kappa$ and $\gamma \gg \Gamma_\perp$), the vibrational mode can be treated as a locale phonon reservoir under the Markov approximation. Going from the Langevin equation of the polarized operator and adiabatically eliminating the degree of freedom of vibrational motion, we formally derive the expression of the average Pauli lowering operator $\langle\sigma_m\rangle$. It is noteworthy that the first term in equation (12) represents a convolution. This character will inspire us to utilize the Laplace transformation (defined as $\langle\bar{f}\rangle(s) = \int_0^\infty \mathrm{d}t\, f(t)e^{-st}$ for the time-dependent function $f(t)$ at $t \geqslant 0$) to simplify the derivation. Then, equation (12) can be reformed as

$$\langle\bar{\sigma}_m\rangle = -ig\bar{\mathcal{F}}_m(s)\langle\bar{a}\rangle, \tag{14}$$

where $\bar{\mathcal{F}}_m$ is the Laplace transform of $\mathcal{F}_m(t)$, expressed as

$$\bar{\mathcal{F}}_m = \sum_k \frac{\lambda^{2k}}{k!}\frac{e^{-\lambda^2}}{s + i(\Delta + k\nu) + (\Gamma_\perp + k\gamma)}, \tag{15}$$

with the Laplace transform variable s. Similarly, taking the average over the cavity field as well as the electronic degrees of freedom on both sides of equation (8*a*), and applying the Laplace transformation, we finally obtain

$$s\langle\bar{a}\rangle = -(i\Delta_c + \kappa)\langle\bar{a}\rangle - ig\sum_m^N \langle\bar{\sigma}_m\rangle + \frac{\eta}{s}. \tag{16}$$

Considering the system with N identical molecules, the Laplace form for the average Pauli lowering operator $\langle\bar{\sigma}_m\rangle$ and the function $\bar{\mathcal{F}}_m(s)$ would be the same for any molecule (m). Combining the Laplace forms of the Pauli operator described by equation (14) and the cavity field illustrated by equation (16), we can get

$$\langle\bar{\sigma}_m\rangle = -\frac{ig\eta\bar{\mathcal{F}}_m}{s[Ng^2\bar{\mathcal{F}}_m + i\Delta_c + \kappa + s]}, \tag{17a}$$

$$\langle\bar{a}\rangle = \frac{\eta}{s[i\Delta_c + s + \kappa + Ng^2\bar{\mathcal{F}}_m]}. \tag{17b}$$

From the final value theorem [37], we get the steady values

$$\langle\sigma_m\rangle_{\mathrm{ss}} = \lim_{s\to 0} s\langle\bar{\sigma}_m\rangle = -\frac{ig\eta\chi}{i\Delta_c + \kappa + Ng^2\chi}, \tag{18a}$$

$$\langle a\rangle_{\mathrm{ss}} = \lim_{s\to 0} s\langle\bar{a}\rangle = \frac{\eta}{(i\Delta_c + \kappa) + Ng^2\chi}, \tag{18b}$$

where 'ss' stands for the steady state situation, and $\chi = \lim_{s\to 0}\bar{\mathcal{F}}_m$. The item $Ng^2\chi$ in equation (18*b*) reflects the hybridization between photonic states and molecular electronic states. One can approximately obtain the hybridized

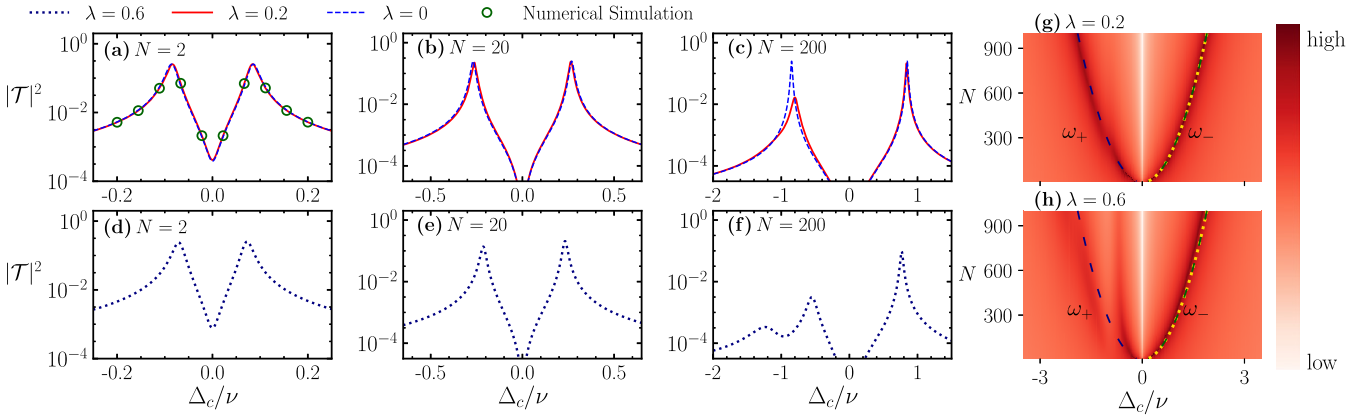

Figure 2. Cavity–molecule spectroscopy. (a)–(f) The influence of the number N (increases as 2, 20, and 200) of identical organic molecules on the intensity of the transmitted field at resonance $\omega_c = \omega_{00}$ at $\lambda = 0$ (blue dashed line), $\lambda = 0.2$ (red solid line), and $\lambda = 0.6$ (black dotted line), respectively. (a) The green circle marks shows the numerical simulation results for $\lambda = 0.2$, $N = 2$ using QuTiP. The intensity of the transmitted field at resonance $\omega_c = \omega_{00}$ as a function of the detuning Δ_c/ν and the number N of organic molecules at $\lambda = 0.2$ (g) and $\lambda = 0.6$ (h), respectively. The spatial intensity profile of the transmitted field is shown in arbitrary units but to scale. The green and blue dashed lines show the frequency shift of the lower and upper polaritonic states versus the number N of organic molecules, respectively, given by equation (19*b*). The frequency shift of the lower polaritonic state is about $\omega_- \approx g\sqrt{N}$ (yellow dotted line). The other parameters are $\nu/\Gamma = 250$, $\Gamma_\phi/\Gamma = 2\kappa_1/\Gamma = 2\kappa_2/\Gamma = 1$, $\gamma/\Gamma = 50$, $g/\Gamma = 5$, and $\eta/\Gamma = 0.01$.

decay rates and frequencies (under resonance conditions, i.e. fixed $\Delta = \Delta_c = 0$) [10, 38]

$$\Gamma_\pm = \frac{\Gamma_{\rm eff} + \kappa}{2} \pm \Re\sqrt{\frac{(\Gamma_{\rm eff} + i\Delta_{\rm eff} - \kappa)^2}{4} - Ng^2}, \tag{19a}$$

$$\omega_\pm = -\frac{\Delta_{\rm eff}}{2} \pm \Im\sqrt{\frac{(\Gamma_{\rm eff} + i\Delta_{\rm eff} - \kappa)^2}{4} - Ng^2}, \tag{19b}$$

where $\Gamma_{\rm eff} = \Re \lim 1/\chi$ and $\Delta_{\rm eff} = \Im \lim 1/\chi$ denote the effective decay rate and additional frequency shift for excitons, respectively.

In experiments, the hybridized decay rates and frequencies can be detected via the cavity transmitted field. According to the input and output relation $a_{2,\rm out}(t) = \sqrt{2\kappa_2}a(t)$, the transmission $\mathcal{T}$ via $\mathcal{T} = \langle a_{2,\rm out}\rangle_{\rm ss}/\langle A_{\rm in}\rangle_{\rm ss}$ in the steady state reign will be expressed as

$$\mathcal{T} = \frac{2\sqrt{k_1 k_2}}{(i\Delta_c + \kappa) + Ng^2\chi}. \tag{20}$$

Figures 2(a)–(f) plot the intensity of the cavity transmission at resonance $\omega_c = \omega_{00}$ in the various numbers N of the organic molecules for the TC (see the blue dashed line) and HTC (see the red solid line and black dotted line) models, respectively. The parameters we have chosen are given in the caption of figure 2, which are associated with recent theoretical research [17, 21, 22, 33]. When multiple molecules emerge in a cavity, the system will be in collective behavior mode with a bright mode that couples to the cavity field with an enhanced strength $g\sqrt{N}$ (for identical molecules). In the limit of $\lambda = 0$, (see the blue dashed line in figures 2(a)–(c)), the cavity transmission will be split into two symmetric peaks with the central frequency separation $2\sqrt{Ng^2 - (\Gamma_\perp + \kappa)^2/4}$ [38–40].

For finite λ, the coupling between electronic states and molecular conformation will produce additional dephasing as well as the frequency shift for excitons, resulting in an asymmetric cavity transmission profile (see the red solid line in figure 2(c) and black dotted line in figures 2(d)–(f)). In the limit of $\lambda^2 \ll 1$ and $g\sqrt{N} \ll \nu$, the evolution of the transmitted field for the HTC model with the detuning Δ_c will exhibit similar behavior to the TC model, due to the small Franck–Condon overlap and the weak collective effects. To clarify the influence of the number N of organic molecules on the hybridized frequencies as well as the decay rates, we numerically show the spatial intensity profile of the transmitted field. It is clear that the evolution of the frequency for the lower polariton with the number N of molecules obeys the rule given by equation (19*b*) (see the green dashed line in figures 2(g) and (h)). For blue-detuned illumination, the spatial intensity profile of the transmitted field seems more complicated (see figures 2(c)–(h)). Typically, when the collective coupling strength $g\sqrt{N} > \nu$ for large Franck–Condon overlap (i.e. $\lambda^2 \sim 1$), one more polaritonic peak appears in the cavity transmission profile (see the black dotted line in figure 2(f)). For the left branch in figure 2(h), the relation between the number N of molecules and the central frequency still obeys the rule given in equation (19*b*) (see the blue dashed line in figure 2(h)). This branch corresponds to the upper polaritons. The appearance of another branch is caused by the perturbation of the excitation state of the vibrational motion, corresponding to the dark polaritonic state [10].

In addition, we would like to point out here that the cavity transmitted field can be used to detect ultra-cold molecules [25]. Considering the presence of rovibrational states, several theoretical studies have modeled one molecule as a several-level system [25, 41]. One can estimate the number of molecules via the frequency separation between upper and lower polaritonic states. In contrast to the previous work [25], the coupling between electronic states and molecular conformation described by the HTC model will make the cavity transmitted field become more complicated (see figures 2(g)

and (h)). Particularly for the large Franck–Conda overlap, it will be a challenging task to detect molecules according to the method introduced by [25] due to the appearance of the peak in the dark polaritonic state and the suppressed intensity of the upper polaritonic state. Notably, a single peak appeared in the spatial intensity profile of the transmitted field when $\Delta_c > 0$, which is associated with the lower polaritons. Considering the relation between the number N of molecules and the central frequency of the lower polaritonic peaks described by equation (19*b*), we can approximately obtain the number of molecules as $N \approx \omega_-^2/g^2$ (see the yellow dotted line in figures 2(g) and (h)).

4. Fluorescence spectrum

In the previous section, we have analyzed the polaritonic features via the transmission field profile. With the increase in the number of molecules, qualitatively different phenomena arise while considering the collective behavior of the emitters. On the other hand, the molecules can interact with each other via the coupling with the quantized cavity field. This will give rise to the modification of the molecular configuration [42], as well as the transition between the electronic ground and excited states. In this section, we will illustrate how the feature is reflected via the fluorescence spectrum.

Before the introduction of the fluorescence spectrum, let us first give the definition of the fluctuation operator. Since the expected values of the Pauli lowering operator $\langle\sigma_m\rangle_{\rm ss}$ and the cavity field $\langle a\rangle_{\rm ss}$ have been obtained in the steady state given by equation (18), one can represent the fluctuation about this steady state using the following operators

$$\begin{aligned}\delta\sigma_m &= \sigma_m - \langle\sigma_m\rangle_{\rm ss}\\ \delta a &= a - \langle a\rangle_{\rm ss}.\end{aligned} \tag{21}$$

Considering the formal solution of the Pauli operator given by equation (9), one can easily derive the expression for the autocorrelation function

$$\begin{aligned}&\langle\delta\sigma_m^\dagger(t)\delta\sigma_m(t+\tau)\rangle\\ &= -ig\int_t^{t+\tau} {\rm d}t_1 {\rm e}^{-(i\Delta+\Gamma_\perp)(t+\tau-t_1)}\langle\delta\sigma_m^\dagger(t)\mathcal{D}_m(t+\tau)\mathcal{D}_m^\dagger(t_1)\langle a\rangle_{\rm ss}\rangle\\ &\quad - ig\int_t^{t+\tau} {\rm d}t_1 {\rm e}^{-({\rm i}\Delta+\Gamma_\perp)(t+\tau-t_1)}\langle\delta\sigma_m^\dagger(t)\mathcal{D}_m(t+\tau)\mathcal{D}_m^\dagger(t_1)\delta a(t_1)\rangle\\ &\quad - \langle\sigma_m\rangle_{\rm ss}\langle\delta\sigma_m^\dagger(t)\rangle + {\rm e}^{-(i\Delta+\Gamma_\perp)\tau}\langle\delta\sigma_m^\dagger(t)\mathcal{D}_m(t+\tau)\mathcal{D}_m^\dagger(t)\sigma_m(t)\rangle.\end{aligned} \tag{22}$$

Under the large vibrational relaxation conditions $\gamma \gg \kappa$ and $\gamma \gg \Gamma$, the correlation time for vibrational motion would be much shorter than the timescale of the correlation between the cavity field and molecules, as well as the intra-molecule correlations. Therefore, the four-operator correlation functions can be separated as

$$\begin{aligned}&\langle\delta\sigma_m^\dagger(t)\mathcal{D}_m(t+\tau)\mathcal{D}_m^\dagger(t_1)\mathcal{O}(t_1)\rangle\\ &\quad\approx \langle\delta\sigma_m^\dagger(t)\mathcal{O}(t_1)\rangle\langle\mathcal{D}_m(t+\tau)\mathcal{D}_m^\dagger(t_1)\rangle\end{aligned} \tag{23}$$

with $\mathcal{O}(t)$ in the set $\{a(t), \sigma_m(t), \sigma_n(t)\}$. In the limit of a long time scale, the system would be in the steady state. Then, the first line in equation (22) can be neglected as the expected value of the fluctuation operator $\langle\delta\sigma_m\rangle_{\rm ss}$ will be zero. The formulation of the desired auto-correlation function is deduced with the convolution integral

$$\begin{aligned}\langle\delta\sigma_m^\dagger(0)\delta\sigma_m(\tau)\rangle_{\rm ss} &= -ig\int_0^\infty {\rm d}t_1\mathcal{F}_m(\tau-t_1)\langle\delta\sigma_m^\dagger(0)\delta a(t_1)\rangle_{\rm ss}\\ &\quad + \langle\delta\sigma_m^\dagger\delta\sigma_m\rangle_{\rm ss}\mathcal{F}_m(\tau),\end{aligned} \tag{24}$$

where $\langle\delta\sigma_m^\dagger(0)\delta\mathcal{O}(\tau)\rangle_{\rm ss} \equiv \lim_{t\to\infty}\langle\delta\sigma_m^\dagger(t)\delta\mathcal{O}(t+\tau)\rangle_{\rm ss}$ and $\langle\delta\sigma_m^\dagger\delta\sigma_m\rangle_{\rm ss} = \langle\sigma_m^\dagger\sigma_m\rangle_{\rm ss} - \langle\sigma_m\rangle_{\rm ss}\langle\sigma_m^\dagger\rangle_{\rm ss}$. Taking the Fourier transformation with the definition $S_{\mathcal{O}}^m(\omega) = \int_{-\infty}^{\infty} {\rm d}\tau\,\langle\delta\sigma_m^\dagger(0)\delta\mathcal{O}(\tau)\rangle_{\rm ss}{\rm e}^{-{\rm i}\omega\tau}$, the correlation function given by equation (24) can be reformed in the Fourier domain, i.e.

$$S_{\sigma_m}^m = -\tilde{\mathcal{F}}_m[igS_a^m - \langle\delta\sigma_m^\dagger\delta\sigma_m\rangle_{\rm ss}], \tag{25}$$

where $\tilde{\mathcal{F}}_m(\omega)$ is the Fourier form for the factor $\mathcal{F}_m(t)$.

Taking the similar method, one can respectively obtain the Fourier forms for the correlation functions $\langle\delta\sigma_m^\dagger(0)\delta\sigma_n(\tau)\rangle_{\rm ss}$ between molecules, and also the correlation function $\langle\delta\sigma_m^\dagger(0)\delta a(\tau)\rangle_{\rm ss}$ between the cavity and molecules

$$\begin{aligned}S_{\sigma_n}^m &= -\tilde{\mathcal{F}}_n(igS_a^m - \langle\delta\sigma_m^\dagger\delta\sigma_n\rangle_{\rm ss}),\\ S_a^m &= -ig\tilde{\mathcal{F}}_a\left(\sum_{n\neq m}^N S_{\sigma_n}^m + S_{\sigma_m}^m\right) + \tilde{\mathcal{F}}_a\langle\delta\sigma_m^\dagger\delta a\rangle_{\rm ss},\end{aligned} \tag{26}$$

where $\langle\delta\sigma_m^\dagger\delta\mathcal{O}\rangle_{\rm ss} = \langle\sigma_m^\dagger\mathcal{O}\rangle_{\rm ss} - \langle\mathcal{O}\rangle_{\rm ss}\langle\sigma_m^\dagger\rangle_{\rm ss}$, and $\tilde{\mathcal{F}}_a(\omega) = 1/[i(\Delta_c+\omega)+\kappa]$.

For identical molecules, the functions $S_{\sigma_n}^m$ $(n \neq m)$ are the same for any molecule pair (m, n) and $S_{\sigma_m}^m$ are interchangeable for any molecule (m). As a result, equations (25) and (26) can be simply reformed as

$$\mathcal{M}_s\boldsymbol{\mathcal{S}}_{\rm Vec} + \boldsymbol{\mathcal{S}}_{\rm in} = 0, \tag{27}$$

with the coefficient matrix

$$\mathcal{M}_s = \begin{pmatrix} -1 & 0 & -ig\tilde{\mathcal{F}}_m\\ 0 & -1 & -ig\tilde{\mathcal{F}}_n\\ -ig\tilde{\mathcal{F}}_a & -i(N-1)g\tilde{\mathcal{F}}_a & -1\end{pmatrix},$$

the vector for the Fourier form of the correlation functions $\boldsymbol{\mathcal{S}}_{\rm Vec} = (S_{\sigma_m}^m, S_{\sigma_n}^m, S_a^m)^{\rm T}$, and the input vector $\boldsymbol{\mathcal{S}}_{\rm in} = (\tilde{\mathcal{F}}_m\langle\delta\sigma_m^\dagger\delta\sigma_m\rangle_{\rm ss}, \tilde{\mathcal{F}}_n\langle\delta\sigma_m^\dagger\delta\sigma_n\rangle_{\rm ss}, \tilde{\mathcal{F}}_a\langle\delta\sigma_m^\dagger\delta a\rangle_{\rm ss})^{\rm T}$. To this end, the solution can be obtained via $\boldsymbol{\mathcal{S}}_{\rm Vec} = -\mathcal{M}_s^{-1}\boldsymbol{\mathcal{S}}_{\rm in}$. It should be noted that the above equation can also be derived by considering the quantum regression theorem. In contrast to traditional methods [43], the convolution integral for $\langle\sigma_m(t)\rangle$ given by equation (12) requires us to get the dynamic equation for the correlation function from the perspective of the frequency domain. In addition, to obtain the value of the vector $\boldsymbol{\mathcal{S}}_{\rm Vec}$, one needs to calculate the expectations $\langle\sigma_m^\dagger\mathcal{O}\rangle$ in the steady state, which have been discussed in appendix C.

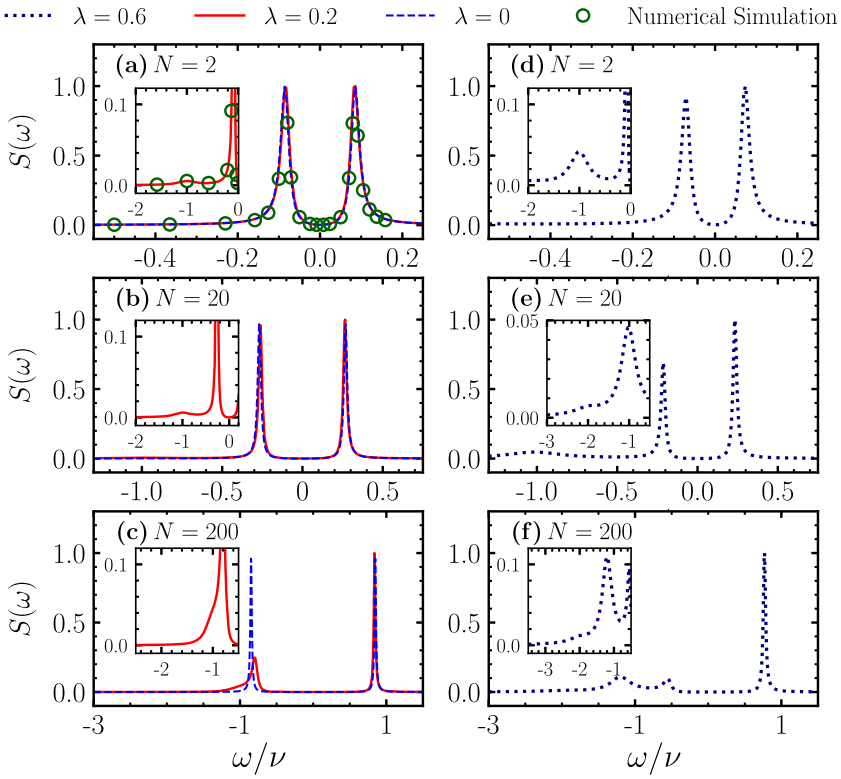

Figure 3. The fluorescence spectrum at resonance $\omega_c = \omega_{00} = \omega_l$ with various numbers N of organic molecules (increases as 2, 20, and 200). We compare the HTC model for different numbers N of molecules against the TC model (blue dashed line) when (a)–(c) $\lambda = 0.2$ and (d)–(f) $\lambda = 0.6$. (a) The green circle markers are numerically calculated using QuTiP for $\lambda = 0.2$ and $N = 2$. The other parameters are the same as in figure 2.

According to the definition of the collective operator $J_- = \sum_{m=0}^{N} \sigma_m$, the fluorescence spectrum in the steady situation can be achieved by taking the Fourier transformation $S = \lim_{t\to\infty} \Re \int_{-\infty}^{\infty} \mathrm{d}\tau \, \langle \delta J_-^\dagger(t) \delta J_-(t+\tau) \rangle \mathrm{e}^{-\mathrm{i}\omega\tau}$. Since $\langle \delta\sigma_m^\dagger(t)\delta\sigma_m(t+\tau)\rangle$, $\langle \delta\sigma_m^\dagger(t)\delta\sigma_n(t+\tau)\rangle$ $(m \neq n)$ are the same for all molecules and all molecular pairs, respectively, we can further get the relation

$$S = N\Re S_{\sigma_m}^m + N(N-1)\Re S_{\sigma_n}^m. \tag{28}$$

Figure 3 illustrates the fluorescence spectrum at resonance $\omega_c = \omega_{00} = \omega_l$. With the number N of molecules increasing, the spectral weight shows some interesting features. In the limit of $\lambda = 0$, the profile for the fluorescence spectrum will exhibit two symmetric peaks with the central frequencies $\omega_\pm$ given by equation (19*b*) (see the blue dashed line). For finite λ, the coupling between electronic and molecular conformation will bring us more amazing phenomena, e.g. the Stokes scatting, the asymmetric profile of the fluorescence spectrum (see the red solid line in figures 3(a)–(c) and the black dotted line in figures 3(d)–(f)). When $N = 2$, one more peak at frequency $\omega = -\nu$ appeared compared with the TC (i.e. $\lambda = 0$) model (see the red solid line in figure 3(a) and the black dotted line in figure 3(d)). This peak corresponds to the Stokes process $|e\rangle|0\rangle_{\mathrm{vib}} \to |g\rangle|1\rangle_{\mathrm{vib}}$, with the transition rate characterized by the Franck–Condon factors ${}_{\mathrm{vib}}\langle 1|\mathcal{D}(\lambda)|0\rangle_{\mathrm{vib}}$ [44]. As the number N of organic molecules increases, the coverage of the Stokes line in the frequency domain will be broadened (see the black dotted line in figures 3(e) and (f)). In particular, at $N = 20$, one can observe that another peak appeared at frequency $\omega = -2\nu$, corresponding to the Stokes process $|e\rangle|0\rangle_{\mathrm{vib}} \to |g\rangle|2\rangle_{\mathrm{vib}}$. The dependence of the profile of the Stokes line on the number of molecules reflects the fact that the molecular conformation has been modified via the collective behavior. When the collective coupling strength $g\sqrt{N} > \nu$, the contribution of the dark polartonic state should be taken into account (see the black dotted line in figure 3(f)), which would result in new physics.

5. Conclusion

In summary, we have studied the collective behavior of organic molecules based on the HTC model. By adiabatically eliminating the degree of freedom of the vibrational motion, we have derived a set of linear equations in the Laplace (or Fourier) domain, involving the Pauli operators, the correlation between the cavity field and molecules, and the correlation between molecules. Based on these equations, we have studied the cavity transmission spectrum for an ensemble of identical organic molecules. Our results reveal that, in contrast to the TC model, the coupling between electronic states and molecular conformation will produce additional dephasing as well as the frequency shift for excitons. This will result in some amazing phenomena, e.g. the suppressed upper polaritonic peak, and the dark polaritonic peak with the central frequency slightly

changed by increasing the number of molecules. In addition, it has been suggested that the cavity transmitted field can detect ultra-cold molecules [25]. Considering the relationship between the hybridized frequencies and the number of molecules, one can estimate the number of molecules via the frequency shift for the lower polaritonic state. Moreover, we also study the steady population in the excited state for total molecules and the fluorescence spectrum. With the number of molecules increasing, the coverage of the Stokes line in the frequency domain is broadened. This means that the probabilities for transition from the electronic excited state to the vibrational excited states in the electronic ground state increased. In other words, the conformation of molecules will be modified due to the collective effects, providing a potential application in the control of the chemical reactivity [11, 12], energy and charge transport [13, 14], and Förster resonance energy transfer [15–17].

Acknowledgments

This work was supported by the Natural Science Foundation of China (under Grant No. 12074030 and No. U1930402). QZ acknowledges fruitful discussions with Lei Du, Yong Li, and Michael Reitz.

Data availability statement

All data that support the findings of this study are included within the article (and any supplementary files).

Appendix A. Dynamic of the vibrational motion

In the limit of weak probe fields $\eta \ll \kappa$, the Heisenberg–Langevin equation for the vibrational motion is given [17] by

$$\frac{\mathrm{d}}{\mathrm{d}t}b = -i(\nu - i\gamma)b + \sqrt{2\gamma}b_{\mathrm{in}}, \tag{A1}$$

where b_{in} is the annihilation operator of thermal noise with zero-average value. The non-vanishing correlation functions are

$$\begin{aligned}\langle b_{\mathrm{in}}^{\dagger}(t)b_{\mathrm{in}}(t_1)\rangle &= \bar{n}_{\mathrm{th}}\delta(t-t_1),\\ \langle b_{\mathrm{in}}(t)b_{\mathrm{in}}^{\dagger}(t_1)\rangle &= (1+\bar{n}_{\mathrm{th}})\delta(t-t_1),\end{aligned} \tag{A2}$$

where $\bar{n}_{\mathrm{th}} = 1/[\exp(\hbar\nu/k_{\mathrm{B}}T_{\mathrm{vib}})] - 1]$ is the average thermal photon numbers at the effective temperature T_{vib}. For brevity, let us assume that the temperature satisfies $k_{\mathrm{B}}T_{\mathrm{vib}}/\hbar\nu \ll 1$. According to the quantum regression theorem [34, 43], the non-zero correlation for the boson operator b at $\tau > 0$ is then obtained

$$\langle b(t)b^{\dagger}(t+\tau)\rangle = \mathrm{e}^{-(\mathrm{i}\nu+\gamma)\tau}. \tag{A3}$$

Introducing the momentum operator $p = i(b^{\dagger} - b)/\sqrt{2}$, one can get its correlation function

$$\langle p(t+\tau)p(t)\rangle = \frac{1}{2}\mathrm{e}^{-(\mathrm{i}\nu+\gamma)\tau}, \tag{A4}$$

and the variance $\langle p^2\rangle(t) = 1/2$. Now, we can get the two-time correlation function for the displacement operator $\mathcal{D} = \exp[\lambda(b - b^{\dagger})] = \exp(i\sqrt{2}\lambda p)$ as

$$\begin{aligned}&\langle \mathcal{D}(t+\tau)\mathcal{D}^{\dagger}(t)\rangle\\ =&\langle \mathrm{e}^{\mathrm{i}\sqrt{2}\lambda p(t+\tau)}\mathrm{e}^{-\mathrm{i}\sqrt{2}\lambda p(t)}\rangle\\ =&\langle \mathrm{e}^{\mathrm{i}\sqrt{2}\lambda[p(t+\tau)-p(t)]}\rangle e^{\lambda^2[p(t+\tau),p(t)]}\\ =&\Big\langle \sum_k \frac{(i\sqrt{2}\lambda)^k}{k!}[p(t+\tau)-p(t)]^k\Big\rangle e^{\lambda^2[p(t+\tau),p(t)]}.\end{aligned} \tag{A5a}$$

Making use of the Isserlis' theorem [22], one can simplify equation (A5*a*) into

$$\begin{aligned}\langle \mathcal{D}(t+\tau)\mathcal{D}^{\dagger}(t)\rangle &= e^{-\lambda^2\langle[p(t+\tau)-p(t)]^2\rangle}e^{\lambda^2[p(t+\tau),p(t)]}\\ &= e^{-\lambda^2[2\langle p^2\rangle - 2\langle p(t+\tau)p(t)\rangle]}\\ &= e^{-\lambda^2}e^{\lambda^2\mathrm{e}^{-(\mathrm{i}\nu+\gamma)(\tau)}}.\end{aligned} \tag{A5b}$$

Similarly, we can also get the four-time correlation function for the displacement operator at $t > t_1 > t_2 > t_3$,

$$\begin{aligned}\langle \mathcal{D}(t)\mathcal{D}^{\dagger}(t_1)\mathcal{D}(t_2)\mathcal{D}^{\dagger}(t_3)\rangle &= \langle \mathrm{e}^{\mathrm{i}\sqrt{2}\lambda p(t)}\mathrm{e}^{-\mathrm{i}\sqrt{2}\lambda p(t_1)}\mathrm{e}^{\mathrm{i}\sqrt{2}\lambda p(t_2)}\mathrm{e}^{-\mathrm{i}\sqrt{2}\lambda p(t_3)}\rangle,\\ &= e^{-\lambda^2\langle[p(t)-p(t_1)+p(t_2)-p(t_3)]^2\rangle}e^{-\lambda^2[p(t)-p(t_1),p(t_2)-p(t_3)]}e^{\lambda^2[p(t),p(t_1)]}e^{\lambda^2[p(t_2),p(t_3)]},\\ &= e^{-2\lambda^2[2\langle p^2\rangle-\langle p(t)p(t_1)\rangle+\langle p(t)p(t_2)\rangle-\langle p(t)p(t_3)\rangle-\langle p(t_1)p(t_2)\rangle+\langle p(t_1)p(t_3)\rangle-\langle p(t_2)p(t_3)\rangle]}\\ &= e^{-2\lambda^2}e^{2\lambda^2\langle p(t)p(t_1)\rangle}e^{-2\lambda^2\langle p(t)p(t_2)\rangle}e^{2\lambda^2\langle p(t)p(t_3)\rangle}e^{2\lambda^2\langle p(t_1)p(t_2)\rangle}e^{-2\lambda^2\langle p(t_1)p(t_3)\rangle}e^{2\lambda^2\langle p(t_2)p(t_3)\rangle}.\end{aligned} \tag{A6a}$$

Submitting equation (A4) into the above equation, and taking the Taylor series expansion, we finally get the expression for the four-time correlation in the sum form

$$\begin{aligned}&\langle\mathcal{D}(t)\mathcal{D}^{\dagger}(t_1)\mathcal{D}(t_2)\mathcal{D}^{\dagger}(t_3)\rangle\\&= e^{-2\lambda^2}\sum_{\{k\}}\frac{(-1)^{k_2+k_5}\lambda^{2\sum_j k_j}}{\prod_j k_j!}\mathrm{e}^{-(k_1+k_2+k_3)(\mathrm{i}\nu+\gamma)(t-t_1)}\\&\times\mathrm{e}^{-(k_2+k_3+k_4+k_5)(\mathrm{i}\nu+\gamma)(t_1-t_2)}\mathrm{e}^{-(\mathrm{k}_3+\mathrm{k}_5+\mathrm{k}_6)(i\nu+\gamma)(\mathrm{t}_2-\mathrm{t}_3)}.\end{aligned}\tag{A6b}$$

Appendix B. Dynamic of electronic states

From the Langevin equation for the cavity field a described by equation (8a), we can take the integration with respect to time to get the formal solution

$$a=\int_0^t \mathrm{d}t_1\,\mathrm{e}^{-(\mathrm{i}\delta_c+\kappa)(t-t_1)}\left[-ig\sum_m\sigma_m(t_1)+\eta+(\sqrt{2\kappa_1}+\sqrt{2\kappa_2})a_{\mathrm{in}}(t_1)\right].\tag{B1}$$

By plugging equation (B1) into the formal solution of the dipole operator $\sigma_m(t)$ described by equation (9) and taking the averages, we find

$$\begin{aligned}\langle\sigma_m\rangle=&-ig\int_0^t\mathrm{d}t_1\int_0^{t_1}\mathrm{d}t_2\mathrm{e}^{-(\mathrm{i}\Delta+\Gamma_\perp)(t-t_1)}\mathrm{e}^{-(\mathrm{i}\Delta_c+\kappa)(t_1-t_2)}\\&\times\langle\mathcal{D}_m(t)\mathcal{D}_m^{\dagger}(t_1)\left[-ig\sum_{n\neq m}^{N}\sigma_n(t_2)-ig\sigma_m(t_2)+\eta\right]\rangle.\end{aligned}\tag{B2a}$$

The item $\langle\mathcal{D}_m(t)\mathcal{D}_m^{\dagger}(t_1\sigma_n(t)\rangle$ reflects the induced interaction between the mth and nth molecule via the quantized cavity field. The item $\langle\mathcal{D}_m(t)\mathcal{D}_m^{\dagger}(t_1)\sigma_m(t_1)\rangle$ relates to the modification of the frequency and decay rate. When we consider the evolution of the Pauli operators, and by submitting equation (9) into equation (B2a), the average value for the Pauli operator is given by

$$\begin{aligned}\langle\sigma_m\rangle=&\,ig^3\sum_{n\neq m}^{N}\int_0^t\mathrm{d}t_1\mathrm{e}^{-(\mathrm{i}\Delta+\Gamma_\perp)(t-t_1)}\int_0^{\mathrm{t}_1}dt_2\mathrm{e}^{-(i\Delta_\mathrm{c}+\kappa)(\mathrm{t}_1-\mathrm{t}_2)}\int_0^{\mathrm{t}_2}dt_3\,\mathrm{e}^{-(i\Delta+\Gamma_\perp)(\mathrm{t}_2-\mathrm{t}_3)}\langle\mathcal{D}_\mathrm{m}(\mathrm{t})\mathcal{D}_\mathrm{m}^{\dagger}(\mathrm{t}_1)\mathcal{D}_\mathrm{n}(\mathrm{t}_2)\mathcal{D}_\mathrm{n}^{\dagger}(\mathrm{t}_3)\mathrm{a}(\mathrm{t}_3)\rangle\\&+ig^3\int_0^t\mathrm{d}t_1\mathrm{e}^{-(\mathrm{i}\Delta+\Gamma_\perp)(t-t_1)}\int_0^{\mathrm{t}_1}dt_2\mathrm{e}^{-(i\Delta_\mathrm{c}+\kappa)(\mathrm{t}_1-\mathrm{t}_2)}\int_0^{\mathrm{t}_2}dt_3\,\mathrm{e}^{-(i\Delta+\Gamma_\perp)(\mathrm{t}_2-\mathrm{t}_3)}\langle\mathcal{D}_\mathrm{m}(\mathrm{t})\mathcal{D}_\mathrm{m}^{\dagger}(\mathrm{t}_1)\mathcal{D}_\mathrm{m}(\mathrm{t}_2)\mathcal{D}_\mathrm{m}^{\dagger}(\mathrm{t}_3)\mathrm{a}(\mathrm{t}_3)\rangle\\&-\eta g\int_0^t\mathrm{d}t_1\int_0^{t_1}\mathrm{d}t_2\mathrm{e}^{-(\mathrm{i}\Delta+\Gamma_\perp)(t-t_1)}\mathcal{D}_m(t)\mathcal{D}_m^{\dagger}(t_1)\mathrm{e}^{-(i\Delta_c+\kappa)(t_1-t_2)}.\end{aligned}\tag{B2b}$$

In the main text, we have roughly taken the Markov approximation (under the large vibrational relaxation condition $\gamma\gg\kappa,\gamma$) to separate the degrees of freedom for the cavity field and vibrational motion as

$$\langle\mathcal{D}_m(t)\mathcal{D}_m^{\dagger}(t_1)a(t_1)\rangle\approx\langle\mathcal{D}_m(t)\mathcal{D}_m^{\dagger}(t_1)\rangle\langle a(t_1)\rangle,\tag{B3a}$$

and also the degrees of freedom for the Pauli operator and vibrational motion as

$$\langle\mathcal{D}_m(t)\mathcal{D}_m^{\dagger}(t_1)\sigma_n(t_1)\rangle\approx\langle\mathcal{D}_m(t)\mathcal{D}_m^{\dagger}(t_1)\rangle\langle\sigma_n(t_1)\rangle.\tag{B3b}$$

This approach implies that we have roughly taken the following approximation

$$\langle\mathcal{D}_m(t)\mathcal{D}_m^{\dagger}(t_1)\mathcal{D}_m(t_2)\mathcal{D}_m^{\dagger}(t_3)\rangle\approx\langle\mathcal{D}_m(t)\mathcal{D}_m^{\dagger}(t_1)\rangle\langle\mathcal{D}_m(t_2)\mathcal{D}_m^{\dagger}(t_3)\rangle.\tag{B4}$$

In this case, all the displacement operators refer to the same vibrational mode. To test the feasibility of this approximation, we undertake further study. According to the expression for the four-time correlation of the displacement operator in equation (A6a), we can take the Laplace transformation for equation (B2b) to obtain

$$\langle\bar{\sigma}_m\rangle=ig^3\sum_{n\neq m}\frac{\bar{\mathcal{F}}_m\bar{\mathcal{F}}_n}{i\Delta_c+\kappa}\langle\bar{a}\rangle+ig^3\bar{\mathcal{F}}_{2,m}\langle\bar{a}\rangle-i\eta g\frac{\bar{\mathcal{F}}_m}{s[i\Delta_c+\kappa]},\tag{B5}$$

where $\bar{\mathcal{F}}_n=\bar{\mathcal{F}}_n$ for identical molecules, and

$$\begin{aligned}\bar{\mathcal{F}}_{2,m}=&\sum_{\{k\}}\frac{1}{\prod_j k_j!}e^{-2\lambda^2}(-1)^{k_2+k_5}\lambda^{2(k_1+k_2+k_3+k_4+k_5+k_6)}\\&\times\frac{1}{[s+i\Delta+i(k_1+k_2+k_3)\nu+(k_1+k_2+k_3)\gamma+\Gamma_\perp][\ldots(1)\ldots][s+i\Delta+i(k_1+k_2+k_3)\nu+(k_1+k_2+k_3)\gamma+\Gamma_\perp]}\end{aligned}\tag{B6}$$

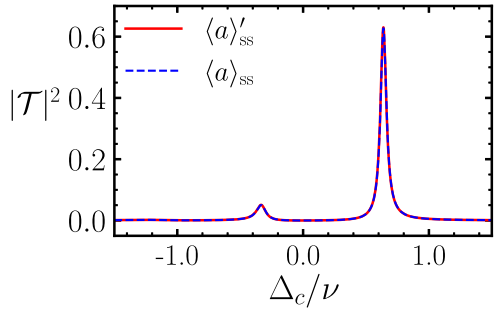

Figure 4. Cavity transmission at resonance $\omega_c = \omega_{00}$ as a function of the detuning Δ_c/ν with the number $N = 200$ of organic molecules at $\lambda = 1$. The data is calculated according to equation (B7) (see the red solid line) and equation (18*b*) (see the blue dashed line), respectively. The other parameters are the same as in figure 2.

with $[\ldots(1)\ldots] = [s + i\Delta_c + i(k_2 + k_3 + k_4 + k_5)\nu + (k_2 + k_3 + k_4 + k_5)\gamma + \kappa]$.

Considering the Laplace form of the cavity field described by equation (16) and using the final value theorem, we finally get

$$\langle a\rangle'_{\rm ss} = \frac{\eta\mathcal{F}_c^0(-1+Ng^2\mathcal{F}_c^0\mathcal{F}_m^0)}{-1+Ng^4\mathcal{F}_c^0[\mathcal{F}_{2,m}^0+(N-1)\mathcal{F}_c^0(\mathcal{F}_m^0)^2]},$$
$$\langle\sigma_m\rangle'_{\rm ss} = -i\eta g\frac{g^2\mathcal{F}_c^0[\mathcal{F}_{2,m}^0+(N-1)\mathcal{F}_c^0(\mathcal{F}_m^0)^2]-\mathcal{F}_c^0\mathcal{F}_m^0}{-1+Ng^4\mathcal{F}_c^0[\mathcal{F}_{2,m}^0+(N-1)\mathcal{F}_c^0(\mathcal{F}_m^0)^2]}. \tag{B7}$$

To verify the validity of the Markov approximation to adiabatically eliminate the degree of freedom of vibrational motion, we plot the cavity transmission spectrum at resonance $\omega_c = \omega_{00}$ with the number $N = 200$ of organic molecules at $\lambda = 1$. As illustrated by figure 4, we can observe that the same behavior is exhibited when we consider the four-time correlation (see the red solid line) or just the two-time correlation (see the blue dashed line).

Appendix C. Steady population

C.1. Dynamics

From the Heisenberg–Langevin equation in equation (7) (or the master equation in equation (6)), we can derive the dynamical equations for the average number of photons in the cavity $\langle n_c\rangle = \langle a^\dagger a\rangle$, and the excited state population for the mth dye molecule $\langle P_m\rangle = \langle\sigma_m^\dagger\sigma_m\rangle$

$$\frac{\rm d}{{\rm d}t}\langle P_m\rangle = -\Gamma_\parallel\langle P_m\rangle - ig(\langle a\sigma_m^\dagger\rangle - \langle a^\dagger\sigma_m\rangle), \tag{C1a}$$

$$\frac{\rm d}{{\rm d}t}\langle n_c\rangle = -2\kappa\langle n_c\rangle - ig\sum_m^N(\langle a^\dagger\sigma_m\rangle - \langle a\sigma_m^\dagger\rangle) + \eta(\langle a\rangle + \langle a^\dagger\rangle), \tag{C1b}$$

where $\Gamma_\parallel = 2\Gamma$ is the longitudinal relaxation rate. By taking the Laplace transformations for equation (C1), we will have the results

$$s\langle\bar P_m\rangle = -\Gamma_\parallel\langle\bar P_m\rangle - ig(\overline{\langle a\sigma_m^\dagger\rangle} - \overline{\langle a^\dagger\sigma_m\rangle}), \tag{C2a}$$

$$s\langle\bar n_c\rangle = -2\kappa\langle\bar n_c\rangle - ig\sum_m^N(\overline{\langle a^\dagger\sigma_m\rangle} - \overline{\langle a\sigma_m^\dagger\rangle}) + \eta(\langle\overline{a}\rangle + \overline{\langle a^\dagger\rangle}). \tag{C2b}$$

The presence of the operator $a^\dagger\sigma_m$ in equation (C2) relates to the nonlinear behavior of the HTC model. In the limit of weak driving $\eta \ll \kappa$, the cavity field in the steady situation is approximately in vacuum. Under this situation, the noise correlation between the cavity field and the molecules as well as the noise correlation between molecules will play important roles. Therefore, we have to give the dynamics equations for the operator $a^\dagger\sigma_m$. While considering the coupling between the electronic states and molecular conformation, we start from the Langevin equation for the cavity filed operator a and the polarized operator $\tilde\sigma_m$, as given in equation (8), to derive the dynamic equation for $a^\dagger\tilde\sigma_m$

$$\begin{aligned}\frac{\rm d}{{\rm d}t}a^\dagger\tilde\sigma_m &= \left(\frac{\rm d}{{\rm d}t}a^\dagger\right)\tilde\sigma_m + a^\dagger\frac{\rm d}{{\rm d}t}\tilde\sigma_m \\ &= [i(\Delta_c-\Delta)-(\kappa+\Gamma_\perp)]a^\dagger\tilde\sigma_m + ig\mathcal{D}_m^\dagger(\sigma_m^\dagger\sigma_m - a^\dagger a) \\ &\quad + ig\mathcal{D}_m^\dagger\sum_{n\neq m}^N\sigma_n^\dagger\sigma_m + \sqrt{2\kappa}A_{in}^\dagger\tilde\sigma_m + \sqrt{2\Gamma_\perp}\mathcal{D}_m^\dagger a^\dagger\sigma_m^{\rm in}.\end{aligned} \tag{C3a}$$

Integrating with respect to the time t on both sides of equation (C3*a*), then the formal solution for the operator $a^\dagger\sigma_m$ will be obtained

$$\begin{aligned}a^\dagger\sigma_m &= \int_0^t{\rm d}t_1{\rm e}^{[{\rm i}(\Delta_c-\Delta)-(\kappa+\Gamma_\perp)](t-t_1)}\mathcal{D}_m(t)\mathcal{D}_m^\dagger(t_1) \\ &\quad\times\{ig[P_m(t_1)-n_c(t_1)]+\eta\sigma_m(t_1)\} \\ &\quad + \mathcal{X}_{m,\rm ind}^t + \mathcal{X}_{m,\rm in}^t,\end{aligned} \tag{C3b}$$

with the dipole–dipole term

$$\begin{aligned}\mathcal{X}_{m,\rm d-d}^t &= ig\int_0^t{\rm d}t_1{\rm e}^{[{\rm i}(\Delta_c-\Delta)-(\kappa+\Gamma_\perp)](t-t_1)} \\ &\quad\times\mathcal{D}_m(t)\mathcal{D}_m^\dagger(t_1)\sum_{n\neq m}^N\sigma_n^\dagger\sigma_m(t_1),\end{aligned} \tag{C3c}$$

and the noise term

$$\begin{aligned}\mathcal{X}_{\rm in}^t &= \int_0^t{\rm d}t_1{\rm e}^{[{\rm i}(\Delta_c-\Delta)-(\kappa+\Gamma_\perp)](t-t_1)}\mathcal{D}_m(t)\mathcal{D}_m^\dagger(t_1) \\ &\quad\times[\sqrt{2\kappa}a_{\rm in}^\dagger\sigma_m(t_1) + \sqrt{2\Gamma_\perp}\mathcal{D}_m^\dagger a^\dagger\sigma_m^{\rm in}(t_1)].\end{aligned} \tag{C3d}$$

Since these individual molecules are introduced to couple a quantized cavity field, an efficient interaction between molecules will be induced, as described by equation (C3*c*). To find the expression of the dipole–dipole term $\mathcal{X}^t_{m,\mathrm{d-d}}$, one needs to consider the expression of $\sigma_n^\dagger\sigma_m$, which can be derived through the following Langevin equation

$$\frac{\mathrm{d}}{\mathrm{d}t}\tilde{\sigma}_n^\dagger\tilde{\sigma}_m = -2\Gamma_\perp\tilde{\sigma}_n^\dagger\tilde{\sigma}_m + ig\mathcal{D}_m^\dagger\mathcal{D}_n(a^\dagger\sigma_m - a\sigma_n^\dagger) + \sqrt{2\Gamma_\perp}\mathcal{D}_m^\dagger\mathcal{D}_n(\sigma_n^\dagger\sigma_m^{\mathrm{in}} + \sigma_n^{\mathrm{in}\dagger}\sigma_m). \tag{C4a}$$

The evolution of $\sigma_n^\dagger\sigma_m(t)$ is then similarly obtained as

$$\sigma_n^\dagger\sigma_m = ig\int_0^t \mathrm{d}t_1 e^{-2\Gamma_\perp(t-t_1)}\mathcal{D}_m(t)\mathcal{D}_m^\dagger(t_1)\left[a^\dagger\sigma_m(t_1) - a\sigma_n^\dagger(t_1)\right]\mathcal{D}_n(t_1)\mathcal{D}_n^\dagger(t) + \mathcal{Y}^t_{\mathrm{in}}, \tag{C4b}$$

with the noise term

$$\mathcal{Y}^t_{\mathrm{in}} = \sqrt{2\Gamma_\perp}\int_0^t \mathrm{d}t_1 e^{-2\Gamma_\perp(t-t_1)}\mathcal{D}_m(t)\mathcal{D}_m^\dagger(t_1)\left[\sigma_n^\dagger\sigma_m^{\mathrm{in}}(t_1) + \sigma_n^{\mathrm{in}\dagger}\sigma_m(t_1)\right]\mathcal{D}_n(t_1)\mathcal{D}_n^\dagger(t). \tag{C4c}$$

From now on, the formal solution for the interactions between the cavity and molecules characterized by equation (C3*b*) as well as the interactions between molecules depicted by equation (C4*b*) have been obtained. To get the excited state population for total molecules, one can take the Markov approximation to adiabatically eliminate the vibrational motion without (or by) submitting equation (C4*b*) into equation (C3*b*), which relates to the perturbative treatment in the first (or second) order.

C.2. Perturbative treatment in the first order

In this subsection, let us take the perturbative treatment in the first order. Under the Markov approximation with the large vibrational relaxation, we can adiabatically eliminate the vibrational motion, as introduced in section 2, to get the dynamic equations for the items $\langle a^\dagger\sigma_m\rangle$ and $\langle\sigma_n^\dagger\sigma_m\rangle$ in the Laplace space

$$\overline{\langle a^\dagger\sigma_m\rangle} = ig\bar{\mathcal{F}}'_m\left(\langle\bar{P}_m\rangle - \langle\bar{n}_c\rangle + \sum_{n\neq m}^{N}\overline{\langle\sigma_n^\dagger\sigma_m\rangle}\right) + \eta\bar{\mathcal{F}}'_m\langle\bar{\sigma}_m\rangle \tag{C5a}$$

$$\overline{\langle\sigma_n^\dagger\sigma_m\rangle} = ig\bar{\mathcal{F}}_{mn}(\overline{\langle a^\dagger\sigma_m\rangle} - \overline{\langle a\sigma_n^\dagger\rangle}), \tag{C5b}$$

where $\bar{\mathcal{F}}'_m$ is the Laplace form for $\mathcal{F}'_m(t) = \exp[(i\Delta_c - i\Delta - \kappa - \Gamma_\perp)t]\langle\mathcal{D}_m(t)\mathcal{D}_m^\dagger(0)\rangle$ with the expression

$$\bar{\mathcal{F}}'_m = \sum_k \frac{\lambda^{2k}}{k!}\frac{e^{-\lambda^2}}{s + i(\Delta - \Delta_c + k\nu) + (\kappa + \Gamma_\perp + k\gamma)}, \tag{C6}$$

and $\bar{\mathcal{F}}_{mn}$ is the Laplace form for $\mathcal{F}_{mn}(t) = \exp(-2\Gamma_\perp t)\langle\mathcal{D}_m(t)\mathcal{D}_m^\dagger(0)\rangle\langle\mathcal{D}_n(0)\mathcal{D}_n^\dagger(t)\rangle$ with the expression

$$\bar{\mathcal{F}}_{mn} = \sum_{k_m,k_n}\frac{\lambda^{2(k_m+k_n)}}{k_m!k_n!}\frac{e^{-2\lambda^2}}{s + i(k_m - k_n)\nu + [2\Gamma_\perp + (k_m + k_n)\gamma]}. \tag{C7}$$

For identical molecules, the Laplace forms for the population of the excited electric state $\overline{\langle\sigma_m^\dagger\sigma_m\rangle}$, the expected value for the interaction between the cavity and molecule $\overline{\langle a^\dagger\sigma_m\rangle}$, as well as the function $\bar{\mathcal{F}}'_m$ are the same as that for any molecule (m), and the expected value for the intra-molecule interaction $\overline{\langle\sigma_n^\dagger\sigma_m\rangle}$, as well as the function $\bar{\mathcal{F}}_{mn}$ are the same for any molecule pair (m, n). As a result, we can simplify equations (C2) and (C5), and transform them into matrix form

$$\mathcal{M}_1\boldsymbol{V}_1 + \eta\boldsymbol{V}_{1,\mathrm{in}} = 0, \tag{C8}$$

with the drift matrix

$$\mathcal{M}_1 = \begin{pmatrix} -2\kappa - s & iNg & -iNg & 0 & 0 \\ ig\bar{\mathcal{F}}'^*_m & -1 & 0 & -ig\bar{\mathcal{F}}'^*_m & -i(N-1)g\bar{\mathcal{F}}'^*_m \\ -ig\bar{\mathcal{F}}'_m & 0 & -1 & ig\bar{\mathcal{F}}'_m & i(N-1)g\bar{\mathcal{F}}'_m \\ 0 & -ig & ig & -\Gamma_\parallel - s & 0 \\ 0 & -ig\bar{\mathcal{F}}_{mn} & ig\bar{\mathcal{F}}_{mn} & 0 & -1 \end{pmatrix}, \tag{C9}$$

the vector $\boldsymbol{V}_1 = (\langle\bar{n}_c\rangle, \overline{\langle a\sigma_m^\dagger\rangle}, \overline{\langle a^\dagger\sigma_m\rangle}, \langle\bar{P}_m\rangle, \overline{\langle\sigma_m^\dagger\sigma_n\rangle})^{\mathrm{T}}$ and the input vector $\boldsymbol{V}_{1,\mathrm{in}} = (\langle\overline{a}\rangle + \overline{\langle a^\dagger\rangle}, \bar{\mathcal{F}}'^*_m\langle\bar{\sigma}_m^\dagger\rangle, \bar{\mathcal{F}}'_m\langle\bar{\sigma}_m\rangle, 0, 0)^{\mathrm{T}}$.

We then obtain the solutions $\boldsymbol{V}_1 = -\eta\mathcal{M}_1^{-1}\boldsymbol{V}_{1,\mathrm{in}}$ by direct matrix inversion. According to the final value theorem, the excited state population for all molecules is finally given by

$$\mathcal{P}_N = \sum_{n=1}^{N}\langle P_m\rangle. \tag{C10}$$

If we set $N = 1$, there will only be one molecule that couples to the cavity and the inter-molecule interaction induced by the cavity (depicted by equation (C3*c*)) can be neglected. In such a situation, the expected value for the excited state population in the steady state will be simplified as

$$\mathcal{P}_1 = \frac{\eta g^2\Re\langle a\rangle_{\mathrm{ss}}\Re\mathcal{F}'^0_m - \eta g\kappa\Im\{\mathcal{F}'^0_m\langle\sigma_m\rangle_{\mathrm{ss}}\}}{\Gamma\kappa + g^2(\Gamma + \kappa)\Re\mathcal{F}'^0_m}, \tag{C11}$$

where $\mathcal{F}'^0_m = \lim_{s\to 0}\bar{\mathcal{F}}'_m$.

Figure 5 illustrates the excited state population for all molecules at resonance $\omega_c = \omega_{00}$ with and without the incoherent coupling between molecules. We compare the HTC model (red solid line) for varying numbers of molecule N against the TC model (blue dashed line) in the limit $\alpha = 0$ (a)–(d) and $\alpha = 1$ (e)–(h). For finite λ, the transfer rate of the population from upper polaritonic states to lower polaritonic states and dark polaritonic states increased with the increasing number of organic molecules. Consequently, the population of the upper polaritonic states will be reduced, and the population of the dark polaritonic states is going to be increased. In addition, the transfer rate for the anti-Stokes process $|g\rangle|0\rangle_{\mathrm{vib}} \to |e\rangle|1\rangle_{\mathrm{vib}}$ is enhanced with the increase in the number N of organic molecules. This reflects the fact that the molecular

conformation has been modified via the collective behavior (figure 6).

C.3. Perturbative treatment in the second order

To test the reasonableness of the approximation as previously mentioned, we will take perturbative treatment in the higher order. Substituting equation (C4*b*) into equation (C3*c*) and taking the averages, we find

$$\begin{aligned}&\langle\mathcal{X}^t_{m,\mathrm{d-d}}\rangle\\ &\approx -g^2\sum_{n\neq m}^{N}\int_0^t \mathrm{d}t_1\int_0^{t_1}\mathrm{d}t_2\,\mathrm{e}^{[\mathrm{i}(\Delta_c-\Delta)-(\kappa+\Gamma_\perp)](t-t_1)}\mathrm{e}^{-2\Gamma_\perp(t_1-t_2)}\\ &\times\langle\mathcal{D}_m(t)\mathcal{D}^\dagger_m(t_2)\rangle\langle\mathcal{D}_n(t_2)\mathcal{D}^\dagger_n(t_1)\rangle[\langle a^\dagger\sigma_m\rangle(t_2)-\langle a\sigma^\dagger_n\rangle(t_2)],\end{aligned}\tag{C12}$$

Here, we have adiabatically eliminated the vibrational motion under the large vibrational relaxation condition (i.e. $\gamma\gg\kappa$ and $\gamma\gg\Gamma$). Noticing that the correlation function $\langle\mathcal{D}_m(t)\mathcal{D}^\dagger_m(t_2)\rangle$ (and $\langle\mathcal{D}_m(t)\mathcal{D}^\dagger_m(t_1)\rangle$) depends on the time difference $t-t_2$ (and $t-t_1$) as described in equation (13), we can reform equation (C12) as

$$\begin{aligned}\langle\mathcal{X}^t_{m,\mathrm{ind}}\rangle &= -g^2e^{-\lambda^2}\sum_{n\neq m}^{N}\int_0^t\mathrm{d}t_1\int_0^{t_1}\mathrm{d}t_2\;\mathrm{e}^{[\mathrm{i}(\Delta_c-\Delta)-(\kappa+\Gamma_\perp)](t-t_1)}\\ &\times\mathrm{e}^{-2\Gamma_\perp(t_1-t_2)}e^{\lambda^2\mathrm{e}^{-(\gamma+\mathrm{i}\nu)(t-t_2)}}\langle\mathcal{D}_n(t_2)\mathcal{D}^\dagger_n(t_1)\rangle\\ &\times[\langle a^\dagger\sigma_m\rangle(t_2)-\langle a\sigma^\dagger_n\rangle(t_2)]\\ &= -g^2\sum_{n\neq m}^{N}\sum_k\int_0^\infty\mathrm{d}t_1\int_0^\infty\mathrm{d}t_2\,\mathcal{F}^{(k)}_m(t-t_1)\mathcal{F}^{(k)}_{mn}(t_1-t_2)\\ &\times[\langle a^\dagger\sigma_m\rangle(t_2)-\langle a\sigma^\dagger_n\rangle(t_2)],\end{aligned}\tag{C13}$$

where $\tilde{\Delta}_k=\Delta_c-\Delta+k\nu$, $\tilde{\Gamma}_{1,k}=\kappa+\Gamma_\perp+k\gamma$, $\tilde{\Gamma}_{2,k}=2\Gamma_\perp+k\gamma$, $\mathcal{F}^{(k)}_m(t)=\Theta(t)\lambda^{2k}\exp(-\lambda^2)\exp[(i\tilde{\Delta}_k-\tilde{\Gamma}_{1,k})t]/k!$, and $\mathcal{F}^{(k)}_{mn}(t_1-t_2)=\Theta(t_1-t_2)\exp[-(ik\nu+\tilde{\Gamma}_{2,k})(t_1-t_2)]\langle\mathcal{D}_n(t_2)\mathcal{D}^\dagger_n(t_1)\rangle$. Since equation (C13) represents a convolution, one can make use of the Laplace transformation to rewrite equation (C12) into the Laplace space:

$$\langle\bar{\mathcal{X}}^t_{m,\mathrm{ind}}\rangle=-g^2\sum_{n\neq m}^{N}\bar{\mathcal{F}}_{mn}[\langle\overline{a^\dagger\sigma_m}\rangle-\langle\overline{a\sigma^\dagger_n}\rangle],\tag{C14}$$

where

$$\begin{aligned}\bar{\mathcal{F}}_{mn}&=\sum_k\bar{\mathcal{F}}^{(k)}_m\bar{\mathcal{F}}^{(k)}_{mn}\\ &=\sum_{k_m,k_n}\frac{\lambda^{2(k_m+k_n)}}{k_m!k_n!}\frac{e^{-2\lambda^2}}{[s+i(\Delta-\Delta_c+k_m\nu)+(\kappa+\Gamma_\perp+k_m\gamma)][s+i(k_m-k_n)\nu+2\Gamma_\perp+(k_m+k_n)\gamma]}.\end{aligned}\tag{C15}$$

By substituting equation (9) into equation (C3*b*), and adiabatically eliminating the degree of freedom of vibrational motion, we similarly obtain the evolution of $\langle a^\dagger\sigma_m\rangle$ in the Laplace space

$$\begin{aligned}\langle\overline{a^\dagger\sigma_m}\rangle &= ig[\bar{\mathcal{F}}'_m(\langle\overline{P}_m\rangle-\langle\bar{n}_c\rangle)-\eta\bar{\mathcal{F}}'_{cm}\langle\bar{a}\rangle]\\ &\quad-g^2\sum_{n\neq m}^{N}\bar{\mathcal{F}}_{mn}[\langle\overline{a^\dagger\sigma_m}\rangle-\langle\overline{a\sigma^\dagger_n}\rangle],\end{aligned}\tag{C16}$$

where $\bar{\mathcal{F}}'_m$ is the Laplace form for $\mathcal{F}'_m(t)=\exp[(i\Delta_c-i\Delta-\kappa-\Gamma_\perp)t]\langle\mathcal{D}_m(t)\mathcal{D}^\dagger_m(0)\rangle$ with the expression

$$\bar{\mathcal{F}}'_m=\sum_k\frac{\lambda^{2k}}{k!}\frac{e^{-\lambda^2}}{s+i(\Delta-\Delta_c+k\nu)+(\kappa+\Gamma_\perp+k\gamma)},\tag{C17}$$

and

$$\bar{\mathcal{F}}'_{cm}=\sum_k\frac{\lambda^{2k}}{k!}\frac{e^{-\lambda^2}}{[s+i(\Delta-\Delta_c+k\nu)+(\kappa+\Gamma_\perp+k\gamma)][s+i(\Delta+k\nu)+(\Gamma_\perp+k\gamma)]}.\tag{C18}$$

For identical molecules, the Laplace forms of the population of the excited electric state $\langle\overline{\sigma^\dagger_m\sigma_m}\rangle$, the expected value of the interaction between the cavity and molecule $\langle\overline{a^\dagger\sigma_m}\rangle$, as well as the function $\bar{\mathcal{F}}'_m$ are the same as that for any molecule (m), and the expected value of the intra-molecule interaction $\langle\overline{\sigma^\dagger_n\sigma_m}\rangle$, as well as the function $\bar{\mathcal{F}}_{mn}$ are the same for any molecule pair (m, n). As a result, we can simplify equations (C2) and (C16) into matrix form

$$\mathcal{M}_2\boldsymbol{V}_2+\eta\boldsymbol{V}_{2,\mathrm{in}}=0,\tag{C19}$$

with the drift matrix

$$\mathcal{M}_2=\begin{pmatrix}-2\kappa-s & -iNg & iNg & 0\\ -ig\bar{\mathcal{F}}'_m & -(N-1)g^2\bar{\mathcal{F}}_{mn}-1 & (N-1)g^2\bar{\mathcal{F}}_{mn} & ig\bar{\mathcal{F}}'_m\\ ig\bar{\mathcal{F}}'^*_m & (N-1)g^2\bar{\mathcal{F}}^*_{mn} & -(N-1)g^2\bar{\mathcal{F}}^*_{mn}-1 & -ig\bar{\mathcal{F}}'^*_m\\ 0 & ig & -ig & -\Gamma_\parallel-s\end{pmatrix},\tag{C20}$$

the vector $\boldsymbol{V}_2=(\langle\bar{n}_c\rangle,\ \langle\overline{a^\dagger\sigma_m}\rangle,\ \langle\overline{a\sigma^\dagger_m}\rangle,\ \langle\bar{P}_m\rangle)^{\mathrm{T}}$ and the input vector $\boldsymbol{V}_{2,\mathrm{in}}=(\langle\bar{a}\rangle+\langle\overline{a^\dagger}\rangle,-ig\bar{\mathcal{F}}'_{cm}\langle\bar{a}\rangle,ig\bar{\mathcal{F}}'^*_m\langle\overline{a^\dagger}\rangle,0)^{\mathrm{T}}$. We then obtain the solutions $\boldsymbol{V}_2=-\eta\mathcal{M}_2^{-1}\boldsymbol{V}_{2,\mathrm{in}}$ by direct matrix inversion. Finally, the excited state population for total molecules is given

$$\mathcal{P}''_N=\sum_{n=1}^{N}\langle P_m\rangle.\tag{C21}$$

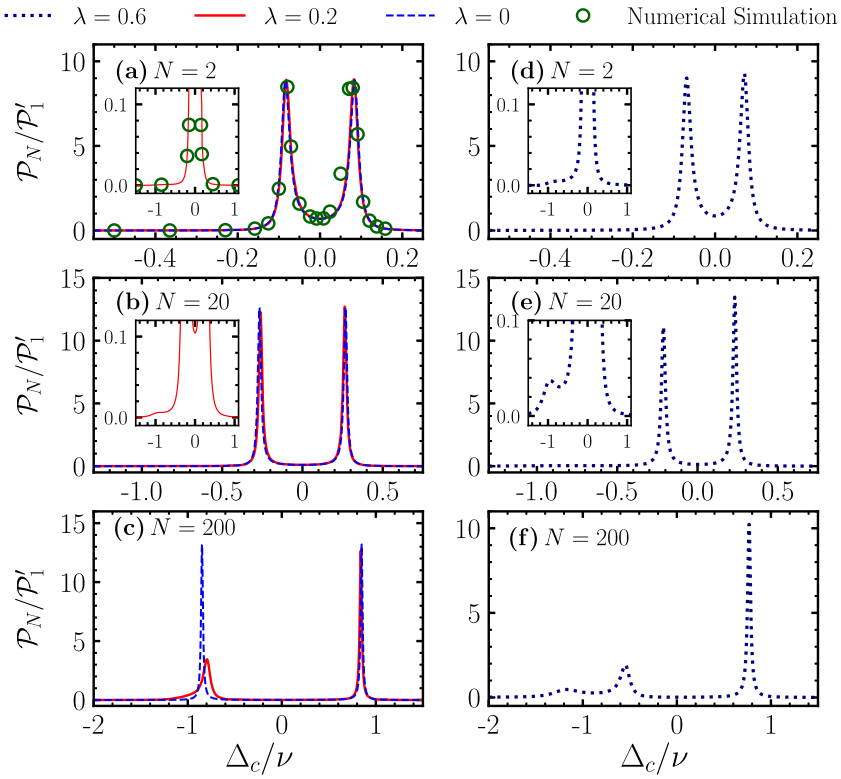

Figure 5. The steady population. The excited state population for all molecules at $\omega_c = \omega_{00}$ in the steady state as a function of the detuning Δ_c/ν with different numbers N (increases as 2, 20 and 200) of organic molecules at $\lambda = 0.6$ (red solid line) and $\lambda = 0$ (blue dashed line) when (a)–(c) $\alpha = 0$ and (d)–(f) $\alpha = 1$. (a), (d) The black dotted line shows the numerical simulation results for $\lambda = 0.6$, $N = 2$ using QuTiP. Here, P_1' is the unit value given by equation (C11) at $\Delta = 0$, $\lambda = 0$. The other parameters are the same as in figure 2.

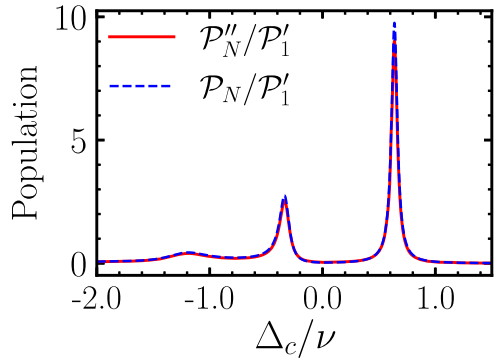

Figure 6. The steady population. The excited state population for total molecules at $\omega_c = \omega_{00}$ in the steady state as a function of the detuning Δ_c/ν with the number $N = 200$ of organic molecules at $\lambda = 1$. We compare the perturbative method in the first order (blue dashed line) against the second order (red solid line). Here, P_1' is the unit value given by equation (C11) at $\Delta = 0$, $\lambda = 0$. The other parameters are the same as in figure 2.

If we set $N = 1$, the expected value of the excited state population in the steady state will be simplified as

$$\mathcal{P}_1'' = \eta g^2 \frac{\Re\langle a\rangle_{\rm ss}\Re\mathcal{F}_m'^0 + \kappa\Re\{\mathcal{F}_{cm}'^0\langle a\rangle_{\rm ss}\}}{\Gamma\kappa + g^2(\Gamma+\kappa)\Re\mathcal{F}_m'^0}, \tag{C22}$$

where $\mathcal{F}_m'^0 = \lim_{s\to 0}\bar{\mathcal{F}}_m'$, and $\mathcal{F}_{cm}'^0 = \lim_{s\to 0}\bar{\mathcal{F}}_{cm}'$.

To test the reasonableness of the Markov approximation to adiabatically eliminate the degree of freedom for the vibrational motion, we plot the excited steady population for total molecules versus the detuning Δ_c/ν at $\omega_c = \omega_{00}$ with the number $N = 200$ of organic molecules at $\lambda = 1$. We can observe that similar behavior is exhibited when we take the perturbative method in the second order (see the red solid line) and the first order (see the blue dashed line).

ORCID iDs

Quansheng Zhang https://orcid.org/0000-0002-9171-8629

References

[1] Klessinger M and Michl J 1995 *Excited States and Photochemistry of Organic Molecules* (New York: Wiley)
[2] Aroca R F 2013 *Phys. Chem. Chem. Phys.* **15** 5355
[3] Doppagne B, Chong M C, Lorchat E, Berciaud S, Romeo M, Bulou H, Boeglin A, Scheurer F and Schull G 2017 *Phys. Rev. Lett.* **118** 127401
[4] Wrigge G, Gerhardt I, Hwang J, Zumofen G and Sandoghdar V 2008 *Nat. Phys.* **4** 60
[5] Kühn S, Håkanson U, Rogobete L and Sandoghdar V 2006 *Phys. Rev. Lett.* **97** 017402
[6] Lidzey D G, Bradley D D C, Skolnick M S, Virgili T, Walker S and Whittaker D M 1998 *Nature* **395** 53
[7] Holmes R J and Forrest S R 2007 *Org. Electron.* **8** 77

[8] Tischler J R, Bradley M S, Bulović V, Song J H and Nurmikko A 2005 *Phys. Rev. Lett.* **95** 036401
[9] Kéna-Cohen S, Davanço M and Forrest S R 2008 *Phys. Rev. Lett.* **101** 116401
[10] Herrera F and Owrutsky J 2020 *J. Chem. Phys.* **152** 100902
[11] Herrera F and Spano F C 2016 *Phys. Rev. Lett.* **116** 238301
[12] Du M, Ribeiro R F and Yuen-Zhou J 2019 *Chem* **5** 1167
[13] Schachenmayer J, Genes C, Tignone E and Pupillo G 2015 *Phys. Rev. Lett.* **114** 196403
[14] Hagenmüller D, Schachenmayer J, Schütz S, Genes C and Pupillo G 2017 *Phys. Rev. Lett.* **119** 223601
[15] Zhong X, Chervy T, Wang S, George J, Thomas A, Hutchison J A, Devaux E, Genet C and Ebbesen T W 2016 *Angew. Chem., Int. Ed.* **55** 6202
[16] Reitz M, Mineo F and Genes C 2018 *Sci. Rep.* **8** 9050
[17] Reitz M, Sommer C and Genes C 2019 *Phys. Rev. Lett.* **122** 203602
[18] Zeb M A, Kirton P G and Keeling J 2018 *ACS Photon.* **5** 249
[19] Klaers J, Schmitt J, Vewinger F and Weitz M 2010 *Nature* **468** 545
[20] May V and Kuhn O 2011 *Charge and Energy Transfer Dynamics in Molecular Systems* 3rd edn (New York: Wiley)
[21] Reitz M, Sommer C, Gurlek B, Sandoghdar V, Martin-Cano D and Genes C 2020 *Phys. Rev. Res.* **2** 033270
[22] Reitz M and Genes C 2020 *J. Chem. Phys.* **153** 234305
[23] Zhang Y, Aizpurua J and Esteban R 2020 *ACS Photon.* **7** 1676
[24] Johansson J R, Nation P D and Nori F 2013 *Comput. Phys. Commun.* **184** 1234
[25] Sawant R, Dulieu O and Rangwala S A 2018 *Phys. Rev.* A **97** 063405
[26] Schwartz T, Hutchison J A, Genet C and Ebbesen T W 2011 *Phys. Rev. Lett.* **106** 196405
[27] Miller W H, Handy N C and Adams J E 1980 *J. Chem. Phys.* **72** 99
[28] Calvo J, Zueco D and Martin-Moreno L 2020 *Nanophotonics* **9** 277
[29] Sánchez-Carrera R S, Delgado M C R, Ferrón C C, Osuna R M, Hernández V, Navarrete J T L and Aspuru-Guzik A 2010 *Org. Electron.* **11** 1701
[30] Herrera F and Spano F C 2017 *Phys. Rev.* A **95** 053867
[31] Herrera F and Spano F C 2018 *ACS Photon.* **5** 65
[32] Ćwik J A, Kirton P, De Liberato S and Keeling J 2016 *Phys. Rev.* A **93** 033840
[33] Arnardottir K B, Moilanen A J, Strashko A, Törmä P and Keeling J 2020 *Phys. Rev. Lett.* **125** 233603
[34] Crispin Gardiner P Z 2004 *Quantum Noise: A Handbook of Markovian and Non-Markovian Quantum Stochastic Methods with Applications to Quantum Optics* (*Springer Series in Synergetics*) 2nd edn (Berlin: Springer)
[35] Nitzan A, Mukamel S and Jortner J 1975 *J. Chem. Phys.* **63** 200
[36] Radonjić M, Kopylov W, Balaž A and Pelster A 2018 *New J. Phys.* **20** 055014
[37] Li J-H, Liu J-B, Chen A-X and Qi C-C 2006 *Phys. Rev.* A **74** 033816
[38] Plankensteiner D, Sommer C, Reitz M, Ritsch H and Genes C 2019 *Phys. Rev.* A **99** 043843
[39] Bernardot F, Nussenzveig P, Brune M, Raimond J M and Haroche S 1992 *Europhys. Lett.* **17** 33
[40] Khitrova G, Gibbs H M, Kira M, Koch S W and Scherer A 2006 *Nat. Phys.* **2** 81
[41] Wellnitz D, Schütz S, Whitlock S, Schachenmayer J and Pupillo G 2020 *Phys. Rev. Lett.* **125** 193201
[42] Galego J, Climent C, Garcia-Vidal F J and Feist J 2019 *Phys. Rev.* X **9** 021057
[43] Carmichael H J 1999 *Statistical Methods in Quantum Optics 1* (*Master Equations and Fokker–Planck Equations, Theoretical and Mathematical Physics*) (Berlin: Springer)
[44] Sauer M, Hofkens J and Enderlein J 2011 *Handbook of Fluorescence Spectroscopy and Imaging: From Single Molecules to Ensembles* (New York: Wiley)